Research Article (Non-Member)

The Functional Integrity of the Shoulder Joint and Pectoralis Major Following Subpectoral Implant Breast Reconstruction[1]

Joshua M. Leonardis[a], Daniel A. Lyons[b], Aviram M. Giladi[c], Adeyiza O. Momoh[b], David B. Lipps 0000-0003-1140-9891[a,d]

[a] School of Kinesiology, University of Michigan, Ann Arbor, MI, USA
[b] Department of Surgery, Section of Plastic Surgery, University of Michigan, Ann Arbor, MI, USA
[c] The Curtis National Hand Center, MedStar Union Memorial Hospital, Baltimore, MD
[d] Department of Biomedical Engineering, University of Michigan, Ann Arbor, MI, USA

Research Article submitted to *Journal of Orthopaedic Research*
Words: ~4400/4200 (Introduction – Discussion)
Figures: 6
Tables: 1
Running title: Functional integrity following breast reconstruction

Author Contributions: Research design: JML, AMG, AOM, DBL; Recruitment: JML, DAL, AOM; Data Acquisition: JML, DAL, DBL; Data Analysis: JML, AOM, DBL; Data Interpretation: JML, DAL, AMG, AOM, DBL; Drafting manuscript: JML, DBL; Revising manuscript: JML, DAL, AMG, AOM, DBL. All authors have read and approved the final submitted manuscript.

Corresponding Author:

David B. Lipps, PhD
401 Washtenaw Ave., CCRB 3730
Ann Arbor, MI 48109
Tel. +1 734-647-3131
Fax. +1 734-936-1925
Email: dlipps@umich.edu

[1] This is the author manuscript accepted for publication and has undergone full peer review but has not been through the copyediting, typesetting, pagination and proofreading process, which may lead to differences between this version and the Version of Record. Please cite this article as doi:10.1002/jor.24257

ABSTRACT

Subpectoral implants for breast reconstruction after mastectomy requires the surgical disinsertion of the sternocostal fiber region of the pectoralis major. This technique is associated with significant shoulder strength and range of motion deficits, but it is unknown how it affects the underlying integrity of the shoulder joint or pectoralis major. The aim of this study was to characterize the long-term effects of this reconstruction approach on shoulder joint stiffness and pectoralis major material properties. Robot-assisted measures of shoulder strength and stiffness and ultrasound shear wave elastography images from the pectoralis major were acquired from 14 women an average of 549 days (range: 313-795 days) post reconstruction and 14 healthy, age-matched controls. Subpectoral implant patients were significantly weaker in shoulder adduction ($p < 0.001$) and exhibited lower shoulder stiffness when producing submaximal adduction torques ($p = 0.004$). The underlying material properties of the clavicular fiber region of the pectoralis major were altered in subpectoral implant patients, with significantly reduced shear wave velocities in the clavicular fiber region of the pectoralis major when generating adduction torques ($p = 0.023$). The clinical significance of these findings are that subpectoral implant patients do not fully recover shoulder strength or stability in the long-term, despite significant recovery time and substantial shoulder musculature left intact. The impact of these procedures extends to the remaining, intact volume of the pectoralis major. Optimization of shoulder function should be a key aspect of the post-reconstruction standard of care.

KEYWORDS

Shoulder mechanics, shoulder stiffness, ultrasound shear wave elastography, muscle mechanics, surgical outcomes

INTRODUCTION

A growing number of women diagnosed with breast cancer will have the disease managed with mastectomy, a surgical procedure that removes all breast tissue. Increasing mastectomy rates have led to a growing number of post-mastectomy breast reconstruction surgeries, with approximately 107,000 such procedures performed annually in the United States[1-5]. Post-mastectomy breast reconstructions are a group of surgical procedures that restore the look and feel of natural breast tissue by utilizing either autologous tissue or an artificial implant. Traditional two-stage subpectoral implant-based breast reconstructions (subpectoral implant) account for nearly 60% of all post-mastectomy breast reconstructions[2; 6]. The first stage of this approach requires the disinsertion of the sternocostal fibers of the pectoralis major (PM) from its attachments on the costal cartilage and lower sternum to allow placement of a tissue expander beneath the muscle. The volume of this expander is increased over several months, thereby stretching the PM to accommodate an implant of the desired size. The second surgical stage is a less extensive procedure whereby the temporary tissue expander is exchanged for a permanent implant.

Disinserting the sternocostal fiber region of the PM can lead to significant long-term functional deficits for patients undergoing post-mastectomy breast reconstruction. The intact PM contributes to shoulder adduction, flexion, and internal rotation[7-9], and as such, its disinsertion results in significant shoulder strength deficits[10]. Adequate PM function is also required for the maintenance of healthy shoulder stability[11-13]. Traditionally, shoulder stability is measured during a clinical assessment by comparing the resistance provided by affected and unaffected shoulders when passively moved through a range of motion. Unfortunately, the subjectivity of clinical assessments of shoulder stability raises concerns regarding their accuracy and repeatability[14-16].

Shoulder stiffness is a biomechanical measure of the resistance of the shoulder to movement, which is key for the execution of activities of daily living[12; 17-24]. Biomechanical measures of shoulder stiffness provide quantitative insights into the net contributions of all soft tissues that stabilize the shoulder. A shoulder with reduced stiffness could be more prone to instability due to less resistance to movement, while a shoulder with enhanced stiffness is resistant to movement and could be prone to disorders like adhesive capsulitis. However, this objective measure cannot differentiate between the contributions of individual soft tissues. Ultrasound shear wave elastography (SWE) can non-invasively estimate the material properties of individual soft tissues *in vivo* in both healthy and clinical populations[25-32]. When collected at rest and during active contraction, shear wave velocity (SWV) provides information regarding the contributions of individual musculature[33]. In combination with objective measures of shoulder stiffness, shear wave elastography provides valuable insight into how subpectoral implant breast reconstruction influences the material properties of the PM.

The primary objective of this study was to determine the effect of subpectoral implant breast reconstruction on the functional integrity of the shoulder joint using objective and reliable robot-assisted measures of shoulder joint strength and stiffness. The secondary objective of this study was to examine how subpectoral implant breast reconstruction influences the material properties of the sternocostal and clavicular fiber regions of the PM at rest and during active contraction. Finally, we assessed the clinical significance of our shoulder strength and stiffness and pectoralis major material properties findings. To achieve these objectives, we acquired robot-assisted biomechanical measures of multidimensional shoulder strength and stiffness, ultrasound SWE-based measures of PM shear wave velocities, and patient-reported outcomes surveys from subpectoral implant breast reconstruction patients and healthy, age-matched

controls. We hypothesized that, when compared to healthy controls, subpectoral implant breast reconstruction patients would exhibit significantly reduced strength in shoulder adduction, flexion, and internal rotation, and significantly reduced shoulder stiffness while producing vertical adduction torques. We further hypothesized that this reduced shoulder strength and stiffness would be driven by underutilization of the PM, which would be evidenced by altered PM material properties. Finally, we hypothesized that reduced shoulder strength and stiffness, and underutilization of the PM would be associated with poorer self-reported upper extremity function.

METHODS

Participants

This was a retrospective cohort study (level of evidence: 3) that investigated the long-term effects of subpectoral implant breast reconstruction on shoulder stiffness and the material properties of the pectoralis major. Twenty-eight women participated in one experimental session each (Table 1). A retrospective chart review from a single surgeon's practice at the University of Michigan was performed to identify women who had previously undergone breast reconstruction between 2014 and 2017. Patients were excluded if they had previously experienced any neuromuscular or orthopaedic disorders affecting the upper limb. Fourteen eligible patients elected to participate. All breast reconstruction patients underwent a two-stage subpectoral implant procedure that required the disinsertion of the sternocostal fiber region of the PM. Fourteen healthy, age-matched women were also recruited from the University of Michigan and Ann Arbor communities. Participants were provided with written consent to procedures

approved by the University of Michigan's Institutional Review Board (HUM00114801 and HUM00111519).

Experimental Setup

In a single visit, participants were secured to a Biodex chair (Biodex Medical Systems, Shirley, New York) with movement restricted using chest and waist straps and cushioned plates positioned along the lower back and sides of their torso. A padded, plastic cast extending from the shoulder to the hand attached the participant's examined shoulder to a computer-controlled brushless servomotor (Baldor Electric Company, Fort Smith, AR) (Figure 1). The affected arm was examined in the subpectoral implant group, which was the dominant limb in 10 of 14 patients. The affected limb was defined as the limb treated for primary breast cancer, or in the case of bilateral breast cancer, the dominant limb was examined. Only the dominant limb was examined in the 14 healthy controls. Within the cast the elbow was fixed at 90°, the wrist was held neutral, and movement of the scapula was unrestricted. The motor's axis of rotation was aligned with the center of rotation of the glenohumeral joint. Shoulder joint torques were measured using a 6DOF load cell (JR3, Inc., Woodland, CA) attached between the motor crank arm and the cast. Our measurement coordinate system utilized established biomechanical standards[34].

Experimental Protocol

Participants performed maximal voluntary contractions (MVC) in the positive and negative directions of plane of elevation (θ), rotation (ϕ), and elevation (Ψ). Values obtained from these contractions were used to normalize the remaining trials to each participant's strength. Participants were then examined in elevation and plane of elevation in a random order. Shoulder posture remained constant (shoulder elevated 90°, flexed 0°) across all trials.

Shoulder joint stiffness was measured in each plane by measuring the resultant shoulder torque. In each measurement plane, the motor applied a series of stochastic perturbations presented as a pseudo-random binary sequence with a 0.06 radian amplitude and 150 millisecond switching interval. These perturbation characteristics were chosen to limit the nonlinearity of muscles, while being able to differentiate between joint dynamics and noise due to muscular activity. Perturbation trials lasted for 60 seconds, during which participants were asked to remain relaxed (0% MVC) or to maintain a constant torque scaled to ±10% MVC in the given measurement plane. Visual feedback was provided in order to assist in the maintenance of the prescribed torque. One trial where the participants remained relaxed was included at the beginning of each configuration to acclimate the participants to the sensation of being perturbed. We repeated each perturbation testing condition for six total trials per measurement plane resulting in 14 perturbation trials.

Following shoulder stiffness trials, an Aixplorer ultrasound elastography machine (Supersonic Imagine, Aix en Provence, France) connected to a SL15-4 linear transducer array (Optimization: Standard, Persistance: Medium, Smoothing: 5, Frame Rate: 12 Hz) was used to perform ultrasound SWE on the PM fiber regions while participants remained relaxed (0% MVC) or maintained a constant torque scaled to 10% MVC in adduction or flexion.

When imaging the clavicular fiber region, the probe was initially placed approximately 1 cm inferior to the clavicle over the midpoint of the muscle. The midpoint of the clavicular fiber region was as identified by the midpoint of a line extending from the sternoclavicular joint to the point on the humerus deep to the anterior deltoid. The probe was then slowly shifted inferiorly from the clavicle until it was located mid-belly. Probe location was established similarly for the sternocostal fiber region. When imaging the sternocostal fiber region, the probe was initially

placed approximately 4 cm inferior to the sternoclavicular joint over the midpoint of the muscle. The probe was then slowly shifted inferiorly from the sternoclavicular joint until it was located mid-belly. The midpoint of the sternocostal fiber region was initially established as the midpoint of a line extending from the xiphoid process to the point on the humerus deep to the anterior deltoid. This midpoint was then adjusted for each participant by shifting the origin of the line superiorly from the xiphoid process based on individual participant's anatomy. The orientation of the transducer was considered satisfactory when individual muscle fascicles could be identified on the B-mode ultrasound image. Each B-mode image was superimposed with an elastography color map (2.5 cm x 1 cm) positioned within the belly of the fiber region of interest (Figure 2). The color map provides calculations of SWV for each pixel. The color map size was constant between participants, but its depth relative to the surface of the skin was adjusted depending on individual anatomy. All images were collected by the same experimenter. The order of all of the trials was randomized. Two images were collected for each fiber region, torque task, and motor configuration, resulting in 24 images per participant.

The breast reconstruction patients also completed the Shoulder Pain and Disability Index (SPADI), which is a 13-item patient-reported outcomes survey that provides insight into the level of shoulder pain and disability experienced by the participant during the execution of activities of daily living in the previous seven days [35].

Data Analysis

Shoulder stiffness was first estimated using a single-input, single-output nonparametric system identification[18; 19; 36]. Impedance was calculated by relating perturbations in direction *i* to the resultant torque response in the same direction. Stiffness was quantified as the frequency

response function H_i between 0 – 10 Hz. This was performed as participants produced torques in one of two different directions: plane of elevation (1) and elevation (2). Nonparametric fits were assessed using variance accounted for (VAF), while partial coherence estimates revealed the frequency ranges where nonparametric fits approximated data well.

$$TQ_\theta(f) = H_\theta(f)\theta(f) \qquad (1)$$

$$TQ_\psi(f) = H_\psi(f)\psi(f) \qquad (2)$$

Frequency response functions were parameterized using a 2nd order linear model consisting of inertial (*I)*, viscous (*B)*, and stiffness (*K)* components (3). These parameters were estimated by substituting $s = i2\pi f$ and fitting a frequency response function with Nelder-Mead non-linear optimization. Only the stiffness component in the specific direction of perturbation (elevation: K_θ, plane of elevation: K_ψ) is reported, as this is the most clinically relevant parameter for assessing shoulder joint stability.

$$H_i(s) = I_i s^2 + B_i s + K_i(s) \quad (3)$$

Shear wave elastography images were analyzed using a custom MATLAB algorithm (Mathworks Inc, Natick, MA, USA) to systematically quantify fiber regions SWVs[30; 31]. This approach began by extracting the SWVs and quality maps for each image. Next, a region of interest within the shear wave color map that corresponded to the muscle alone was manually selected. This ensured that the aponeurosis or other tissues did not bias the data. Depending on individual anatomy, the size of this region of interest differed slightly image to image. The quality map determined the accuracy of our SWV measures pixel by pixel within the region of interest. The quality map reflects the manufacturer's calculation regarding the cross-correlation of shear waves propagating within the tissue. Finally, the algorithm computed the mean SWV for each image from the pixels that possessed a quality map above the 0.7 threshold. The mean

SWVs obtained from the two images collected for each fiber region, torque task, and motor configuration are reported.

An external trigger was utilized to obtain an elastography image and collect a two second buffer of torque data (one second prior to and one second after the trigger). Torque data were analyzed in MATLAB, where they were low-pass filtered at 500 Hz with a 6th-order analog Bessel filter and averaged across each 2-s trial. The torque data were then normalized as a percentage of the maximum torque produced for each specific experimental motor configuration.

Statistical Analysis

All statistical procedures were performed in SPSS (v24, IBM Corporation, Chicago, IL, USA). Differences in demographic measures (age, height, mass, BMI) between our experimental groups were investigated using t-tests. We tested our first hypothesis that subpectoral implant patients would exhibit significantly reduced shoulder strength. Using independent t-tests we evaluated the maximum isometric voluntary strength between patients and controls in six separate directions. Significance was set at an adjusted p-value of 0.0083 for these six comparisons using Bonferroni correction. We tested our hypothesis that subpectoral implant patients would exhibit significantly reduced shoulder stiffness using a separate two-way ANOVA for stiffnesses in each measurement plane (elevation, plane of elevation). Our outcome measure was stiffness, while torque task (at rest, ± elevation, and ± plane of elevation) and experimental group (subpectoral implant and healthy control) were fixed factors. We tested our hypothesis that subpectoral implant patients would exhibit altered pectoralis major material properties using a three-way ANOVA, where SWV was the outcome measure and fiber region (clavicular, sternocostal), torque task (rest, flexion, adduction), and experimental group were

fixed factors. Bonferroni corrections for multiple comparisons were used for post hoc analyses. We tested our hypothesis that reduced shoulder strength and stiffness, and underutilization of the pectoralis major would be associated with poorer patient-reported outcomes using a forced-entry regression analysis where SPADI score was the dependent variable and measures of shoulder strength and stiffness, and PM material properties were independent variables. ANOVAs and regression analyses utilized a significance level of $p<0.05$. Observed power is reported for all significant findings.

RESULTS

Demographics

No significant differences in age ($t_{26} = -1.136$, $p = 0.27$), height ($t_{26} = -0.265$, $p = 0.79$), weight ($t_{26} = 1.325$, $p = 0.20$), or BMI ($t_{26} = 1.805$, $p = 0.09$) existed between the experimental groups. The subpectoral implant reconstruction patients were evaluated an average (SD) of 549 (39) days post-operatively.

Multidimensional Shoulder Strength and Stiffness

The subpectoral implant group was significantly weaker in adduction than controls ($t_{26} = -3.765$, $p = 0.001$, $power = 0.943$) (Figure 2). The subpectoral implant patients were also weaker in internal rotation ($t_{26} = -2.105$, $p = 0.045$), but this did not reach statistical significance after controlling for multiple strength comparisons. There were no significant differences between groups when producing maximal abduction ($t_{26} = -0.930$, $p = 0.361$), flexion ($t_{26} = -0.898$, $p = 0.377$), extension ($t_{26} = -0.108$, $p = 0.915$), or external rotation ($t_{26} = -1.428$, $p = 0.165$) torques.

Shoulder Stiffness

System identification of shoulder joint stiffness allowed us to uncover inherent differences in the mechanical integrity of the shoulder between subpectoral implant patients and healthy controls. Figure 3 shows frequency response functions and 2nd order linear model fits for representative subpectoral implant and control participants. Stiffness is represented by the model fit as it approaches 0 Hz. The representative participant from each experimental group exhibited similar shoulder stiffness while at rest (Figure 3A) as evidenced by similar model fits between 0-10 Hz. As the participants produced volitional shoulder adduction torque (Figure 3B), the healthy participants exhibited noticeably greater shoulder stiffness when compared to the subpectoral implant patients. Overall, these system identification methods were robust, as the model fits were able to account for 87 ± 9% of all variance in experimental torque across all subjects and stiffness trials.

There was a main effect of experimental group on shoulder stiffness when participants were perturbed in elevation, with the subpectoral group exhibiting significantly reduced shoulder stiffness ($F_{1,1} = 9.005$, $p = 0.004$, $power = 0.842$). There was also a main effect of task on shoulder stiffness in elevation ($F_{1,2} = 47.769$, $p < 0.001$, $power = 1$). Specifically, stiffnesses during adduction and abduction were similar to one another ($p = 0.798$), but both were significantly greater than stiffness at rest (adduction: $p < 0.001$, flexion: $p < 0.001$). Multiple comparisons showed that the subpectoral implant group exhibited 45.1% lower shoulder stiffness when compared to healthy controls while generating vertical adduction torques ($p = 0.001$) (Figure 4). Multiple comparisons also revealed a difference between the groups when producing abduction torques, but did not reach statistical significance ($p = 0.09$).

When participants were perturbed in the plane of elevation, there was a main effect of task ($F_{1,2} = 27.040$, $p < 0.001$, $power = 1$), but not group ($F_{1,1} = 1.257$, $p = 0.266$). Similar to

findings from elevation, shoulder stiffness during flexion and extension were similar to one another ($p = 1.000$), but both were significantly greater than stiffness at rest (adduction: $p < 0.001$, flexion: $p < 0.001$).

Pectoralis Major Fiber Region Material Properties

There was a main effect of experimental group ($F_{1,1} = 6.257$, $p = 0.013$, $power = 0.701$) on SWVs, with the healthy group exhibiting significantly greater SWVs than the subpectoral implant group. There was also a main effect of task ($F_{1,2} = 58.063$, $p < 0.001$, $power = 1$) on SWVs, with SWVs greater during adduction than at rest, and greater during flexion than during adduction. Additionally, there was a main effect of region ($F_{1,1} = 40.290$, $p < 0.001$, $power = 1$) on SWVs, with the clavicular fiber region exhibiting significantly greater SWVs than the sternocostal fiber region. Finally, there was a region × task interaction ($F_{1,2} = 9.031$, $p < 0.001$, $power = 0.972$), with the fiber regions of the pectoralis major exhibiting unique material properties depending on torque task (Figure 5).

Post hoc analyses revealed that in both experimental groups, SWVs were greater in the clavicular region than in the sternocostal fiber region during flexion (subpectoral: $p = 0.001$, healthy: $p < 0.001$) (Figure 6). In the healthy group, SWVs were also greater in the clavicular fiber region during adduction ($p = 0.046$). There were no differences between the fiber regions at rest in either group (subpectoral: $p = 0.309$, healthy: $p = 0.232$) and the subpectoral group did not exhibit between fiber region differences during adduction ($p = 0.210$).

The experimental groups utilized the fiber regions of the pectoralis major differently (Figure 6). When producing 10% MVC adduction torques, the subpectoral implant group exhibited 15.0% lower SWVs in the clavicular region than the healthy group ($p = 0.023$). There was also a trend toward significance in the sternocostal fiber during flexion ($p = 0.056$), with the

healthy group exhibiting 12.9% greater SWVs than the subpectoral implant group. No between group differences existed in the clavicular ($p = 0.505$) or sternocostal ($p = 0.398$) fiber regions when at rest. Similarly, no between group differences existed in the clavicular fiber region during flexion ($p = 0.247$), or in the sternocostal fiber region during adduction ($p = 0.124$).

Patient-Reported Outcomes

In the subpectoral implant group, several measures of shoulder joint integrity and PM material properties reached clinical significance. Decreasing shoulder abduction strength ($r = -0.679$, $p = 0.022$) as well as decreasing shoulder stiffness as patients generated adduction ($r = -0.729$, $p = 0.013$) and abduction torques ($r = -0.729$, $p = 0.013$) was associated with increasing SPADI score, which indicates greater shoulder pain and disability. Furthermore, increasing SWV in the clavicular ($r = 0.673$, $p = 0.023$) and sternocostal ($r = 0.642$, $p = 0.031$) fiber regions of the PM when patients were at rest were associated with increasing SPADI scores. No other metrics of shoulder joint integrity or PM material properties reached statistical significance.

DISCUSSION

This study evaluated the joint and tissue-level implications of two-stage subpectoral implant breast reconstruction, which is the most commonly used post-mastectomy breast reconstruction procedure. Our results provide the first objective evidence that this reconstruction approach compromises the functional integrity of the shoulder joint by reducing shoulder strength and stiffness when compared to healthy age-matched controls. Our results indicate that this reconstruction approach alters function of the remaining, intact clavicular fiber region of the PM. Our results also show that patient-reported measures of shoulder strength and disability can

be captured using objective and repeatable measures of shoulder strength and stiffness, and PM material properties.

Isometric measures of shoulder strength provide insights into the level of impairment experienced by subpectoral implant breast reconstruction patients. To date, only a single investigation has attempted to do so in this patient population[10]. Their results suggest that the disinsertion of the sternocostal fiber region of the PM during subpectoral implant breast reconstruction causes significant reductions in shoulder flexion, adduction, and internal rotation strength. However, the applications of their findings are limited, as their patient population was less than one year post-reconstruction, and their control participants were significantly younger than their patient population. Our use of age-matched controls and patients further removed from reconstruction provide more robust insights into the long-term implications of these surgeries. Clinical practice assumes that, given enough time to recover, the musculoskeletal system adequately compensates for the removal of shoulder musculature[37]. The subpectoral implant patients included in the current study were, on average, 20 months post-surgery. Despite this recovery period, 13 out of 14 subpectoral implant participants exhibited maximal shoulder adduction torques below the healthy control group mean, while 10 out of 14 exhibited maximal shoulder internal rotation torques below the mean for the healthy group. Our results suggest that compensatory mechanisms may not fully restore shoulder strength in this patient population.

The current study was the first to use novel, repeatable measures of shoulder stiffness to confirm that subpectoral implant breast reconstruction compromises the functional integrity of the shoulder joint. These measures of stiffness quantify a patient's ability to maintain shoulder joint stability, which provides insights into shoulder function during dynamic tasks such as activities of daily living[24]. In a single posture with the arm elevated 90 degrees, we found that

both subpectoral implant patients and healthy controls exhibited similar shoulder stiffness at rest in both elevation and plane of elevation. These results are to be expected, as muscle constitutes a small contribution to overall joint stiffness at rest[38]. When producing volitional joint torques, shoulder stiffness is maintained almost entirely by the coordinated activations of shoulder musculature[38-40]. We found that subpectoral implant patients were unable to maintain shoulder joint stiffness when producing submaximal vertical adduction torques. These results confirm those from an investigation utilizing subjective patient-reported data that found approximately 50% of pectoralis major flap patients will experience altered shoulder stiffness[41]. Reductions in shoulder stiffness during vertical adduction could affect a variety of activities of daily living, include reaching for objects on a table. Interestingly, shoulder stiffness while producing submaximal flexion torques was not affected by the surgical disinsertion of the sternocostal region of the PM. It has been hypothesized that the clavicular, not the sternocostal fiber region, is responsible for maintaining shoulder joint stiffness in the plane of elevation[35]. Our results suggest that the intact clavicular fiber region of the PM sufficiently maintains shoulder stiffness in the plane of elevation in the absence of a portion of the sternocostal fiber region.

Our use of shear wave elastography allowed us to further investigate the tissue-level implications of subpectoral implant breast reconstruction on the material properties of the PM. We obtained SWE measurements from both fiber regions of the PM during submaximal torque generation and rest. The healthy control group exhibited similar SWVs between the fiber regions at rest, and greater SWVs in the clavicular fiber region during both adduction and flexion. The subpectoral implant group differed, as it exhibited greater SWVs in the clavicular fiber region at rest and during the generation of adduction torques, and similar between-region SWVs during the generation of flexion torques. Furthermore, we observed that when producing adduction

torques, subpectoral implant patients exhibit significantly lower SWVs in the clavicular fiber region than the healthy controls. Together, these results suggest that the clavicular fibers region of the pectoralis major in subpectoral implant patients contributes more to joint stiffness at rest and during the generation of flexion torques, while it reduces its contributions to adduction torques. However, both fiber regions of the pectoralis major are being underutilized in subpectoral implant patients when compared to healthy controls. These findings contrast previous data that showed increased activity in the clavicular fiber region post-reconstruction when compared to pre-reconstruction levels during maximal voluntary contractions [42]. Future work should further investigate the long-term neuromuscular adaption of shoulder musculature to subpectoral implant breast reconstruction.

The Shoulder Pain and Disability Index clarified if the significant functional deficits identified here had an impact on a patient's activities of daily living. We found that decreasing shoulder strength and stiffness was associated with increased shoulder pain and disability. These results suggest that interventions that increase shoulder strength and stability may be beneficial for reducing post-operative patient complications. We also found that increased pectoralis major SWVs were associated with increased shoulder pain and disability. Shear wave velocity holds a strong relationship with shear modulus, and is often used as a proxy for soft tissue stiffness[43; 44]. These findings suggest that reducing PM tissue stiffness may have a positive effect on breast reconstruction patients shoulder pain and disability during the execution of activities of daily living.

This study had certain limitations. Our study design did not allow us to account for the longitudinal effects of the disinsertion of the PM. We were also unable to control for the volume of muscle disinserted. We attempted to curtail this limitation by using a clinical population

recruited from a single surgeon's clinic, which would insure that the procedure was performed similarly across all patients. Our testing procedures included just a single shoulder posture. This posture was chosen as it places the moment arm of both fiber regions of the PM at an optimal magnitude[7]. Finally, a single volitional torque magnitude was used for all shoulder stiffness and shear wave elastography trials. This level was chosen in an attempt to reduce the effects of fatigue. Finally, it is unknown if patients with changes in muscle material properties observed with ultrasound SWE had underlying fatty degeneration driving these changes, as the current study did not have access to magnetic resonance imaging scans for each participant.

In conclusion, subpectoral implant patients experience long-term and potentially chronic deficits in shoulder strength when compared to healthy controls. Robot-assisted measures of shoulder joint stiffness indicated subpectoral implant patients do not fully recover shoulder stability, despite prolonged recovery time and substantial shoulder musculature left intact. We also observed chronic changes to the material properties of the remaining intact fiber regions of the pectoralis major following subpectoral implant breast reconstruction. Finally, many of our measures of shoulder strength and stiffness, and pectoralis major material properties were of clinical significance. In recent years, a pre-pectoral option for implant-based breast reconstruction has been introduced in order to avoid the disinsertion of the PM. The primary reason for this reconstruction option however has not been to address functional problems, but to address patient complaints of animation deformities of the breast that occur with PM contraction over implants[45; 46]. Our results suggest that when possible, consideration should be given to pre-pectoral implant placement in order to avoid functional deficits arising from the disinsertion of the pectoralis major. Additionally, these results place a greater emphasis on the need to develop

targeted interventions to pre- and post-operatively rehabilitate breast cancer patients that opt for an implant-based subpectoral post-mastectomy breast reconstruction.

ACKNOWLEDGEMENTS

The study was financially supported by a Susan G. Komen Clinical Fellowship (D.B.L), a Plastic Surgery Foundation pilot grant (A.O.M), and the University of Michigan Comprehensive Cancer Center Fund for Discovery (D.B.L. and A.O.M.). The authors thank Thomas Olinger, Brian Diefenbach, and Amani Alkayyali for their assistance with data collection.

References

1. 2017. 2017 National Clearinghouse of Plastic Surgery. In: Surgeons ASoP editor.
2. Albornoz CR, Bach PB, Mehrara BJ, et al. 2013. A paradigm shift in US Breast reconstruction: increasing implant rates. Plastic and reconstructive surgery 131:15-23.
3. Hernandez-Boussard T, Zeidler K, Barzin A, et al. 2013. Breast reconstruction national trends and healthcare implications. The breast journal 19:463-469.
4. Jagsi R, Jiang J, Momoh AO, et al. 2014. Trends and variation in use of breast reconstruction in patients with breast cancer undergoing mastectomy in the United States. Journal of Clinical Oncology 32:919.
5. Kummerow KL, Du L, Penson DF, et al. 2015. Nationwide trends in mastectomy for early-stage breast cancer. JAMA surgery 150:9-16.
6. Cemal Y, Albornoz CR, Disa JJ, et al. 2013. A paradigm shift in US breast reconstruction: Part 2. The influence of changing mastectomy patterns on reconstructive rate and method. Plastic and reconstructive surgery 131:320e-326e.
7. Ackland DC, Pak P, Richardson M, et al. 2008. Moment arms of the muscles crossing the anatomical shoulder. Journal of Anatomy 213:383-390.
8. Kuechle DK, Newman SR, Itoi E, et al. 1997. Shoulder muscle moment arms during horizontal flexion and elevation. Journal of Shoulder and Elbow Surgery 6:429-439.
9. Langenderfer J, Jerabek SA, Thangamani VB, et al. 2004. Musculoskeletal parameters of muscles crossing the shoulder and elbow and the effect of sarcomere length sample size on estimation of optimal muscle length. Clinical Biomechanics 19:664-670.
10. de Haan A, Toor A, Hage JJ, et al. 2007. Function of the pectoralis major muscle after combined skin-sparing mastectomy and immediate reconstruction by subpectoral implantation of a prosthesis. Annals of plastic surgery 59:605-610.
11. Halder A, Zhao K, O'driscoll S, et al. 2001. Dynamic contributions to superior shoulder stability. Journal of Orthopaedic Research 19:206-212.
12. Labriola JE, Lee TQ, Debski RE, et al. 2005. Stability and instability of the glenohumeral joint: the role of shoulder muscles. Journal of shoulder and elbow surgery 14:S32-S38.

13. Veeger H, Van Der Helm F. 2007. Shoulder function: the perfect compromise between mobility and stability. Journal of biomechanics 40:2119-2129.
14. Hegedus EJ, Goode A, Campbell S, et al. 2007. Physical examination tests of the shoulder: a systematic review with meta-analysis of individual tests. British journal of sports medicine.
15. Hegedus EJ, Goode AP, Cook CE, et al. 2012. Which physical examination tests provide clinicians with the most value when examining the shoulder? Update of a systematic review with meta-analysis of individual tests. Br J Sports Med 46:964-978.
16. Wright AA, Wassinger CA, Frank M, et al. 2012. Diagnostic accuracy of scapular physical examination tests for shoulder disorders: a systematic review. Br J Sports Med:bjsports-2012-091573.
17. Halder A, Zhao KD, O'driscoll S, et al. 2001. Dynamic contributions to superior shoulder stability. Journal of Orthopaedic Research 19:206-212.
18. Perreault EJ, Kirsch RF, Acosta AM. 1999. Multiple-input, multiple-output system identification for characterization of limb stiffness dynamics. Biological cybernetics 80:327-337.
19. Perreault EJ, Kirsch RF, Crago PE. 2001. Effects of voluntary force generation on the elastic components of endpoint stiffness. Experimental Brain Research 141:312-323.
20. Pouliart N, Gagey O. 2005. Significance of the latissimus dorsi for shoulder instability. I. Variations in its anatomy around the humerus and scapula. Clinical Anatomy 18:493-499.
21. Holzbaur KR, Murray WM, Delp SL. 2005. A model of the upper extremity for simulating musculoskeletal surgery and analyzing neuromuscular control. Annals of biomedical engineering 33:829-840.
22. Hogan N. 1985. The mechanics of multi-joint posture and movement control. Biological cybernetics 52:315-331.
23. McIntyre J, Mussa-Ivaldi F, Bizzi E. 1996. The control of stable postures in the multijoint arm. Experimental brain research 110:248-264.
24. Rancourt D, Hogan N. 2001. Stability in force-production tasks. Journal of motor behavior 33:193-204.
25. Chernak L, DeWall R, Lee K, et al. 2013. Length and activation dependent variations in muscle shear wave speed. Physiological measurement 34:713.
26. Gennisson J-L, Deffieux T, Macé E, et al. 2010. Viscoelastic and anisotropic mechanical properties of in vivo muscle tissue assessed by supersonic shear imaging. Ultrasound in medicine and biology 36:789-801.
27. Koo TK, Guo J-Y, Cohen JH, et al. 2014. Quantifying the passive stretching response of human tibialis anterior muscle using shear wave elastography. Clinical biomechanics 29:33-39.
28. Kwon DR, Park GY, Lee SU, et al. 2012. Spastic cerebral palsy in children: dynamic sonoelastographic findings of medial gastrocnemius. Radiology 263:794-801.
29. Lacourpaille L, Hug F, Bouillard K, et al. 2012. Supersonic shear imaging provides a reliable measurement of resting muscle shear elastic modulus. Physiological measurement 33:N19.
30. Lee SS, Gaebler-Spira D, Zhang L-Q, et al. 2016. Use of shear wave ultrasound elastography to quantify muscle properties in cerebral palsy. Clinical Biomechanics 31:20-28.
31. Lee SS, Spear S, Rymer WZ. 2015. Quantifying changes in material properties of stroke-impaired muscle. Clinical Biomechanics 30:269-275.

32. Shinohara M, Sabra K, Gennisson JL, et al. 2010. Real-time visualization of muscle stiffness distribution with ultrasound shear wave imaging during muscle contraction. Muscle & nerve 42:438-441.
33. Bercoff J, Tanter M, Fink M. 2004. Supersonic shear imaging: a new technique for soft tissue elasticity mapping. IEEE transactions on ultrasonics, ferroelectrics, and frequency control 51:396-409.
34. Wu G, Van der Helm FC, Veeger HD, et al. 2005. ISB recommendation on definitions of joint coordinate systems of various joints for the reporting of human joint motion—Part II: shoulder, elbow, wrist and hand. Journal of biomechanics 38:981-992.
35. Roach KE, Budiman-Mak E, Songsiridej N, et al. 1991. Development of a shoulder pain and disability index. Arthritis & Rheumatism: Official Journal of the American College of Rheumatology 4:143-149.
36. Lipps DB, Baillargeon EM, Ludvig D, et al. 2015. System identification of multidimensional shoulder impedance during volitional contractions. IFAC-PapersOnLine 48:1369-1374.
37. Spear SL, Hess CL. 2005. A review of the biomechanical and functional changes in the shoulder following transfer of the latissimus dorsi muscles. Plastic and reconstructive surgery 115:2070-2073.
38. Bigliani LU, Kelkar R, Flatow EL, et al. 1996. Glenohumeral Stability: Biomechanical Properties of Passive and Active Stabilizers. Clinical Orthopaedics and Related Research (1976-2007) 330:13-30.
39. Blasier R, Soslowsky L, Malicky D, et al. 1997. Posterior glenohumeral subluxation: active and passive stabilization in a biomechanical model. JBJS 79:433-440.
40. Hu X, Murray WM, Perreault EJ. 2011. Muscle short-range stiffness can be used to estimate the endpoint stiffness of the human arm. Journal of neurophysiology 105:1633-1641.
41. Refos JW, Witte BI, de Goede CJ, et al. 2016. Shoulder morbidity after pectoralis major flap reconstruction. Head & neck 38:1221-1228.
42. Hage JJ, van der Heeden JF, Lankhorst KM, et al. 2014. Impact of combined skin sparing mastectomy and immediate subpectoral prosthetic reconstruction on the pectoralis major muscle function: a preoperative and postoperative comparative study. Annals of plastic surgery 72:631-637.
43. Gennisson J-L, Catheline S, Chaffaı S, et al. 2003. Transient elastography in anisotropic medium: application to the measurement of slow and fast shear wave speeds in muscles. The Journal of the Acoustical Society of America 114:536-541.
44. Gennisson J-L, Deffieux T, Macé E, et al. 2010. Viscoelastic and anisotropic mechanical properties of in vivo muscle tissue assessed by supersonic shear imaging. Ultrasound in medicine & biology 36:789-801.
45. Reitsamer R, Peintinger F. 2015. Prepectoral implant placement and complete coverage with porcine acellular dermal matrix: a new technique for direct-to-implant breast reconstruction after nipple-sparing mastectomy. Journal of Plastic, Reconstructive & Aesthetic Surgery 68:162-167.
46. Sigalove S, Maxwell GP, Sigalove NM, et al. 2017. Prepectoral implant-based breast reconstruction: rationale, indications, and preliminary results. Plastic and reconstructive surgery 139:287-294.

Figure 1: Schematic of experimental setup. A single-axis rotary motor perturbed a participant's examined shoulder in one plane of motion while a six-degree-of-freedom load cell measured resultant torques in all three dimensions. Visual feedback was provided via LCD screen. (A) The rotary motor was positioned to move the arm in the vertical plane while participants were relaxed or generating shoulder torques in ± elevation. (B) The rotary motor was positioned to move the arm in the horizontal plane while participants were relaxed or generating shoulder torques in ± plane of elevation.

Figure 2: Representative frequency response functions (Light Gray) relating the torque response (Black) to a 1-D perturbation (Dark Gray). Figure 2A presents data from one participant from each experimental group while those participants remained relaxed. Figure 2B presents data when those same participants produced volitional shoulder torque scaled to +10% MVC adduction. Participants were perturbed for 60 seconds total, but only 10 seconds of data are shown. A 2nd order approximation to the frequency response functions is represented as dashed black lines. Stiffness is represented by the model fit between 0-10 Hz.

Figure 3: Participants performed maximal isometric shoulder torques in the positive and negative directions in the elevation (adduction, abduction), plane of elevation (flexion, extension), and rotation planes (internal rotation, external rotation). Bars represent mean ± standard error isometric shoulder strength (Nm) error for each experimental group. * denotes significant difference at $p < 0.05$.

Figure 4: Participants were perturbed in elevation (A) and plane of elevation (B). During perturbation trials, participants were asked to remain relaxed (Rest) or to maintain torques scaled to -10% MVC (Adduction/Flexion) and +10% MVC (Abduction/Extension) in each plane of

motion. Bars represent mean ± standard error shoulder stiffness (Nm/rad) for each experimental group. * denotes significant difference at $p < 0.05$.

Figure 5: Approximate probe placement over the clavicular and sternocostal fiber regions of the pectoralis major. Representative B-Mode ultrasound images with shear wave elastography color map for each experimental group (subpectoral implant, healthy control) during each prescribed torque task (at rest, 10% MVC adduction, 10% MVC flexion).

Figure 6: Between group differences in the material properties of the fiber regions of the pectoralis major. During SWE trials, participants remained relaxed (Rest) or produced volitional joint torques scaled to +10% MVC elevation and plane of elevation. Error bars represent mean ± standard error shear wave velocity (m/s) for each experimental group. * denotes significant between group difference. † denotes significant within group difference for the subpectoral implant group. ‡ denotes significant within group difference for the healthy control group. All significances are at the $p < 0.05$ level.

Table 1. Mean (standard error) participant demographics for each experimental group. Group differences were explored using t-tests. * denotes a significant difference at $p < 0.05$.

	Subpectoral	Healthy Control	*p*
Number of Participants	14	14	

Age (yrs)	49 (2.6)	53 (1.3)	0.27
Height (m)	1.64 (.01)	1.64 (.02)	0.79
Weight (kg)	71 (3.4)	65 (3.0)	0.20
BMI (kg/m^2)	26 (1.3)	24 (0.71)	0.09
Days Post-Operative	549 (39)		
Dominant/Non-Dominant Limb	10/4		
Radiation Therapy (Yes/No)	0/14		
Chemotherapy (Yes/No)	5/9		
Axillary Lymph Node Dissection (Yes/No)	0/14		
Sentinel Lymph Node Dissection (Yes/No)	12/14		

Table 1. Mean (standard error) participant demographics for each experimental group. Group differences were explored using t-tests. * denotes a significant difference at $p < 0.05$.

	Subpectoral	Healthy Control	*p*
Number of Participants	14	14	
Age (yrs)	49 (2.6)	53 (1.3)	0.27

Height (m)	1.64 (.01)	1.64 (.02)	0.79
Weight (kg)	71 (3.4)	65 (3.0)	0.20
BMI (kg/m^2)	26 (1.3)	24 (0.71)	0.09
Days Post-Operative	549 (39)		
Dominant/Non-Dominant Limb	10/4		
Radiation Therapy (Yes/No)	0/14		
Chemotherapy (Yes/No)	5/9		
Axillary Lymph Node Dissection (Yes/No)	0/14		
Sentinel Lymph Node Dissection (Yes/No)	12/14		

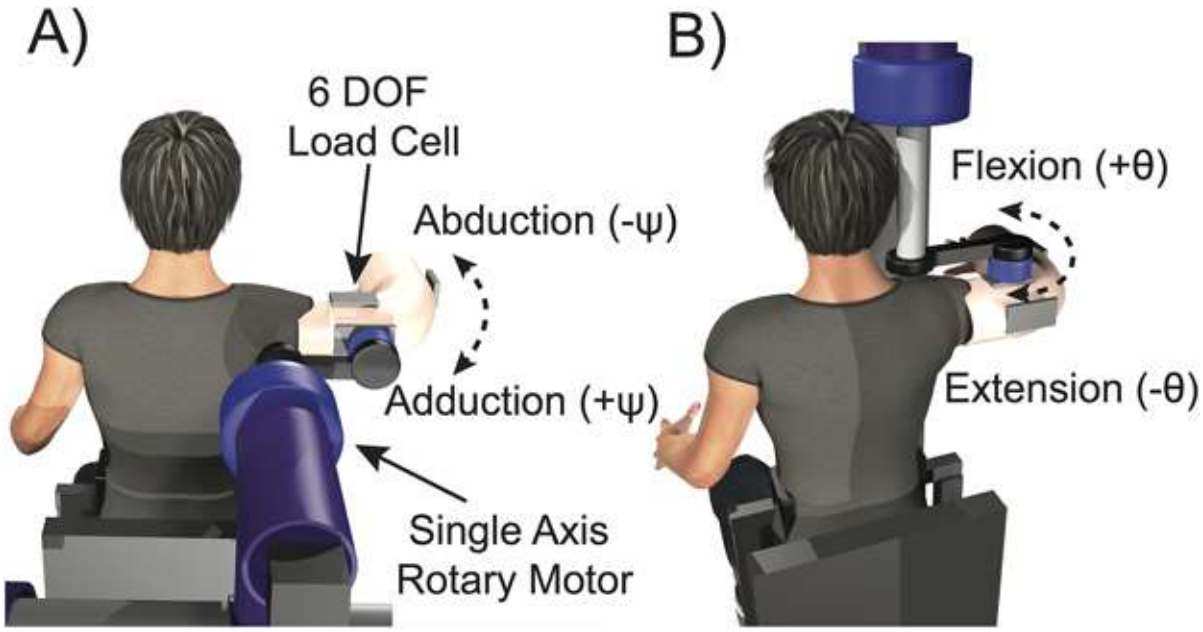

Figure 1

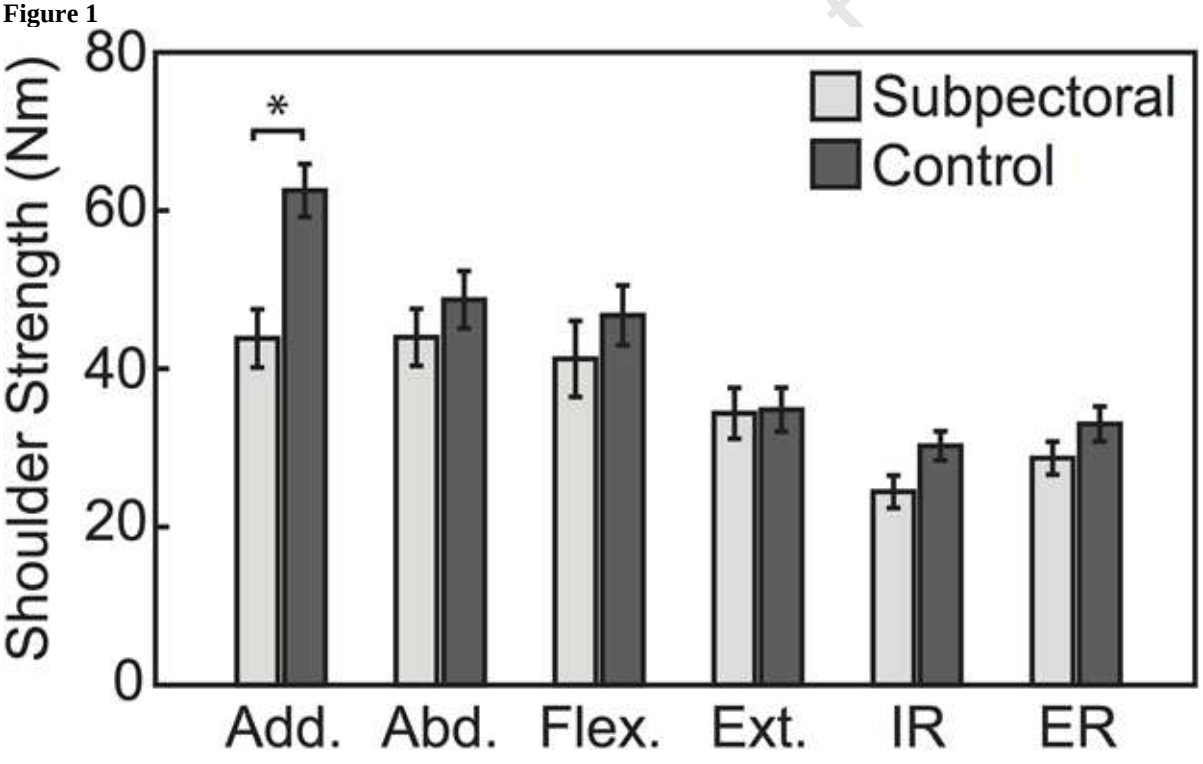

Figure 2

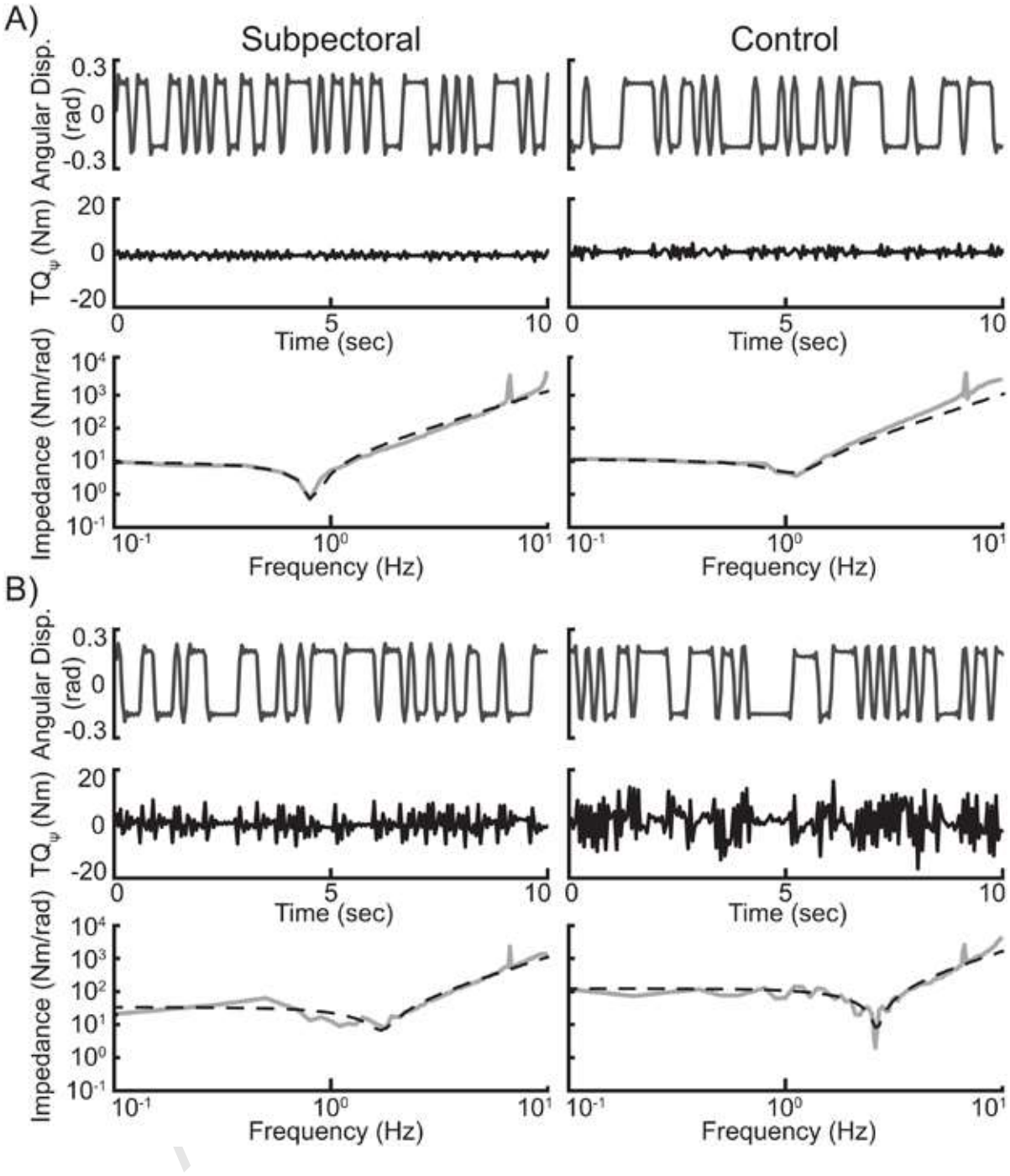
A)
Subpectoral
Control
Angular Disp. (rad)
0.3
0
-0.3
TQψ (Nm)
20
0
-20
0
5
10
Time (sec)
Impedance (Nm/rad)
10⁴
10³
10²
10¹
10⁰
10⁻¹
10⁻¹
10⁰
10¹
Frequency (Hz)
B)
Angular Disp. (rad)
TQψ (Nm)
Time (sec)
Impedance (Nm/rad)
Frequency (Hz)

Figure 3

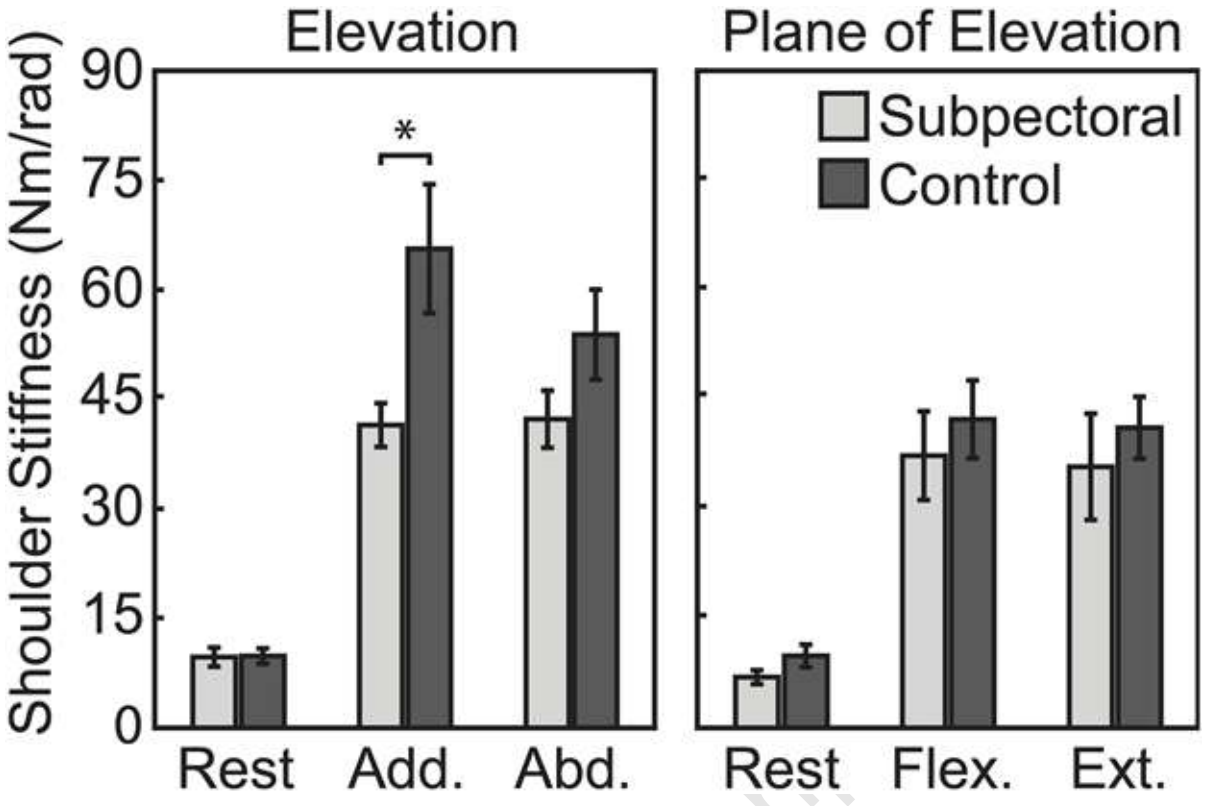

Figure 4

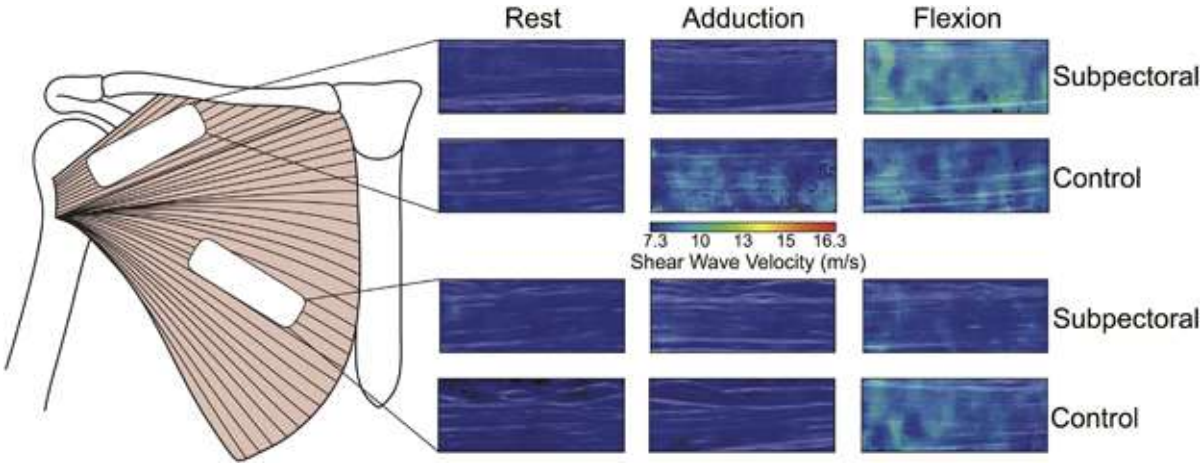

Figure 5

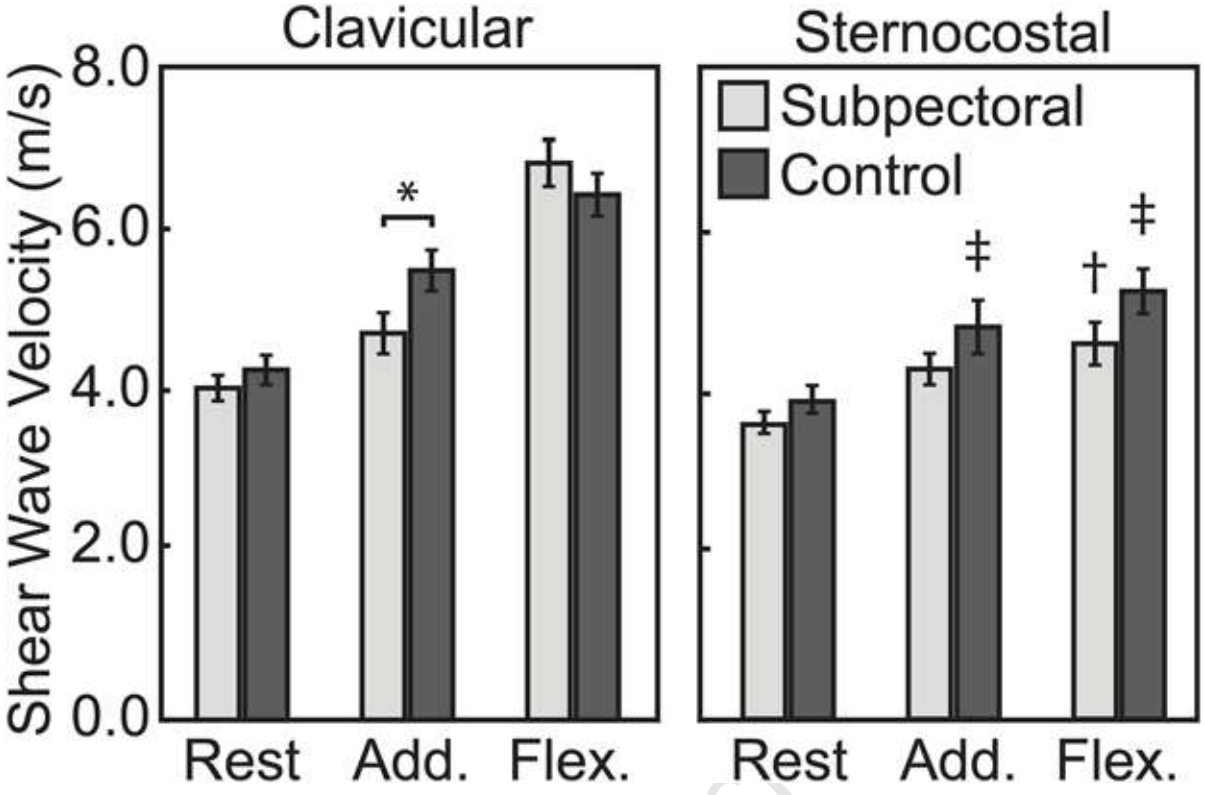

Figure 6